2-Aryl-3H-indol-3-ones: Synthesis, electrochemical behaviour and antiplasmodial activities

5 AUTHORS, INCLUDING:

Ennaji Najahi

Paul Sabatier University - Toulouse III

12 PUBLICATIONS   **28** CITATIONS

SEE PROFILE

Alexis Valentin

Paul Sabatier University - Toulouse III

143 PUBLICATIONS   **2,282** CITATIONS

SEE PROFILE

Paul-Louis Fabre

Paul Sabatier University - Toulouse III

72 PUBLICATIONS   **717** CITATIONS

SEE PROFILE

Karine Reybier

Paul Sabatier University - Toulouse III

31 PUBLICATIONS   **665** CITATIONS

SEE PROFILE

Short communication

2-Aryl-3H-indol-3-ones: Synthesis, electrochemical behaviour and antiplasmodial activities

Ennaji Najahi [a,b,*], Alexis Valentin [a,b], Paul-Louis Fabre [a,b], Karine Reybier [a,b,1], Françoise Nepveu [a,b,1]

[a] Université de Toulouse III, UPS, PHARMA-DEV, UMR 152, 118 Route de Narbonne, F-31062 Toulouse Cedex 9, France
[b] IRD, UMR 152, F-31062 Toulouse Cedex 9, France

ABSTRACT

The synthesis of indolone derivatives and their antiplasmodial activity in vitro against Plasmodium falciparum at the blood stage are described. The 2-aryl-3H-indol-3-ones were synthesized via deoxygenation of indolone-N-oxides. Electrochemical behaviour, antiplasmodial activity and cytotoxicity on human tumor cell lines were compared to those of indolone-N-oxides. The antiplasmodial IC_{50} (concentrations at 50% inhibition) of these compounds ranged between 49 and 1327 nM. Among them, the 2-(4-dimethylaminophenyl)-5-methoxy-indol-3-one, **7**, had the best antiplasmodial activity in vitro (IC_{50} = 49 nM; FcB1 strain) and selectivity index (SI (CC_{50} MCF7/IC_{50} FcB1) = 423.4). Thus, the hits identified in this deoxygenated series correspond to their structural homologs in the N-oxide series with comparable electrochemical behaviour at the nitrogen–carbon double bond.

© 2014 Elsevier Masson SAS. All rights reserved.

1. Introduction

Of the different Plasmodium species causing malaria in humans, Plasmodium falciparum and Plasmodium vivax are the two most prevalent species responsible for this disease [1]. Because of the resistance of malaria parasites to current antimalarial drugs, new structurally diverse drugs are needed to prepare the next generation of treatments. In this long-term drug discovery task, the use of the erythrocytic stage of P. falciparum is convenient to carry out large-scale phenotypic whole-cell-based screening [2,3].

In our previous studies, we identified several hits among the indolone-N-oxide series [4,5] and we recently demonstrated that albumin-bound nanoparticles of the practically water-insoluble antimalarial lead greatly enhanced its efficacy [6]. The formulation achieved a complete cure of Plasmodium berghei-infected mice at 25 mg/kg with an inhibition of parasitemia (99.1%) comparable to that of artesunate and chloroquine and it was remarkably effective not only in prolonging survival time but also in inhibiting recrudescence. In 'humanized' mice infected with P. falciparum, the same dose of nanoparticles proved to be highly effective, with parasitemia

reduced by 97.5%, and the mean survival time prolonged. We also demonstrated that the strong antiplasmodial activities of these compounds were related to their oxido-reductive properties interfering with the redox mechanisms of the parasitized host cell as a consequence of the P. falciparum metabolism. Electrochemical analysis shows that the first electron transfer recorded during the first reduction process corresponds to the reduction of the carbon–nitrogen bond (O=N=C to O•N–C⁻) and that this first reduction potential is structurally connected to the IC_{50} values against P. falciparum (FcB1) [7,8]. In the host cells, healthy and Pf-infected-RBC (pRBC), the bioreduction is thiol- and enzyme-dependent giving an active reduced metabolite (a dihydro-derivative) that has been isolated and identified [9]. This bioreduction activates a Syk kinase which results in a dramatic rise in band 3 tyrosine phosphorylation in pRBC [10]. This triggers complete dissociation of ankyrin from band 3 leading to membrane vesiculation and loss of membrane surface area until the explosion of the Pf-infected-RBC and parasite death. These links between antimalarial activity and drug bioreducibility have encouraged the search for new types of compounds with comparable chemical properties [11,12].

In the present study, we chose to synthesize the deoxygenated form of indolone-N-oxides and compare the electrochemical behaviour and antiplasmodial activities of 2-aryl-3H-indol-3-ones versus 2-aryl-3H-indol-3-one-N-oxides whose structures are given in Fig. 1.

* Corresponding author. University Paul Sabatier, Faculty of Pharmacy, PHARMA-DEV, 118 Route de Narbonne, F-31062 Toulouse Cedex 9, France.
E-mail addresses: ennaji.najahi@univ-tlse3.fr, najahimco@yahoo.fr (E. Najahi).
[1] These authors contributed equally to the work.

2. Results and discussion

2.1. Chemistry

A simple and inexpensive procedure for the deoxygenation of indolone-*N*-oxides **g** [4,13,14] with indium trichloride in acetonitrile at ambient pressure gives the 2-aryl-3*H*-indol-3-ones **1**–**9**. The procedure gives high yields of deoxygenated products [15]. The compounds synthesized are reported in Table 1. The synthesis of the indolone-*N*-oxide derivatives **g** is divided into two sub-steps: the first involves *Sonogashira* coupling of 2-halo-nitroaryls **d** with an alkyne **c**, followed by the nitro-alkyne cycloisomerization of the *o*-alkynylnitrobenzenes **f** in the presence of catalytic amounts of Pd(CH$_3$CN)$_2$Cl$_2$ in acetonitrile under reflux [16]. Compounds **d** were obtained by electrophilic nitration of *o*-bromoaryl aldehydes **e** using a fuming nitric acid/acetic acid mixture [5]. Synthesis of 1-alkynes **c** involved the preparation of 1-(trimethylsilyl)-alkynes **b** [17,18] *via Sonogashira* coupling, followed by a desilylation step [17,19] (Scheme 1).
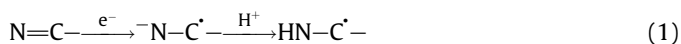
The compounds were chemically characterized by chromatography (TLC and HPLC), infrared (IR), NMR (^{1}H and ^{13}C), MS and HRMS. The IR spectra showed bands in the range of 1720–1730 cm^{-1} which confirmed the presence of a C=O function. In the ^{13}C NMR spectra, the most significant information was the appearance of signals at $\delta = 192$–194 ppm indicating the presence of the carbonyl function of the indol-3-one ($\delta = 186$–188 ppm, indolone-*N*-oxides). The mass spectra showed the respective [M+H]$^+$ peaks. Log P_{calc} values (Table 1) calculated with the VCCLAB software [20] range between 2.64 and 3.51 with compound **8** being the most lipophilic in the series, and **6**, the least. Going from 2-aryl-3*H*-indol-3-one-*N*-oxides to 2-aryl-3*H*-indol-3-ones by deoxygenation led to an increase of the lipophilicity with log P_{calc} values increasing about 0.7–0.8. The same tendency between the two series was observed on the IC$_{50}$ values (*Pf*-FcB1 strain) meaning a slight decrease of the activity in this new series except for compounds **3** and **5**.

2.2. Electrochemistry

Fig. 3 represents the voltammograms recorded in acetonitrile for compound 7 and its *N*-oxide form 7′ (Fig. 2) at a potential scan speed of 0.1 V/s. The electrochemical behaviour is similar and characterized by a first electron transfer more or less reversible, around −0.8 V, followed by a second irreversible electron transfer at −1.72 V for 7 and −1.67 V for 7′ (Fig. 3b). This irreversible reduction was attributed to the C=O function while the reversible electron transfer concerned the N=C bond of the indolone core [7]. When the potential scan is restricted to the first reduction (Fig. 3a), whatever is the compound, the electron transfer is reversible and is monoelectronic by reference to ferrocene. The standard potential are calculated by E° = ½(Ep$_{forward}$ + Ep$_{backward}$): −0.798 V for 7 and −0.793 V for 7′ which means that the electron transfer on the N=C bond is unaffected by the N−O bond in the oxygenated form 7′. Due to the reversibility of this electron transfer, even at low scan speed, the

the produced radical anion produced is stable within the time scale of cyclic voltammetry.

So, EPR spectroscopy was coupled with electrolyses in the EPR cell. The EPR spectra confirmed the formation of radical-anions. The corresponding EPR spectra and corresponding simulations are presented in Fig. 4. The reduction of **7** at −1 V gives rise to the formation of a radical characterised by the hyperfine splitting constants $a_N = 2.55$ G, $a_{N'} = 2.5$ G, $a_H = 0.8$ G, $a_{2H} = 0.4$ G, $a_{2H'} = 0.6$ G. The constants are in favour of the formation, after reduction, of a C2 carbon centred radical, the hydrogen coupling would in this case be attributable to the 4 hydrogen of the phenyl ring (a_{2H} and $a_{2H'}$) and to the N1(H) formed after protonation of N1 (Eq (1)). Whereas the nitrogen coupling would correspond to N1 (a_N) and to the nitrogen of the dimethylamino group ($a_{N'}$). In the case of 7′ as described previously [7], the radical formed corresponds to the nitroxide anion radical characterised by a triplet ($a_{N1} = 5.9$ G) (Eq. (2)). The C2 centred radical formed from C2 is relatively stable few minutes after the end of the electrolysis, whereas the nitroxide radical formed by reduction of 7′ is unstable and disappear immediately after the end of the electrolysis.

$$N{=}C{-}\xrightarrow{e^-}{}^-N{-}\overset{\bullet}{C}{-}\xrightarrow{H^+}HN{-}\overset{\bullet}{C}{-} \quad (1)$$

$$O^-{-}N^+{=}C\xrightarrow{e^-}O^\bullet{-}N{-}C^- \quad (2)$$

2.3. Biology

The nine compounds were evaluated *in vitro* for their antiplasmodial activity against the chloroquine resistant FcB1 strain of *P. falciparum* together with their cytotoxicity against the MCF7 cell line to determine their selectivity index (CC$_{50}$MCF-7/IC$_{50}$FcB1). The results were compared with those of the indolone-*N*-oxide series (Table 1, Fig. 1).

The non-substituted compound (2-phenylindol-3-one **1**; R^1 = R^2 = H) had the lowest antiplasmodial activity (IC$_{50} = 1327$ nM) in the series. Replacement of R^2 (H) by groups having a mesomeric effect (+M: OCH$_3$, Cl, OH) improved the activity (IC$_{50}$/nM: **2** = 514, **3** = 192, **4** = 101). Replacement of R^1 (H) by methoxy group improved the activity (IC$_{50}$ = 141 nM). Placing a methoxy group at R^1 and at R^2 a methoxy, dimethylamino, isopropoxy or hydroxyl group leads to the best activities in this series (IC$_{50}$/nM: **6** = 80, **7** = 49, **8** = 88, **9** = 99). It appeared that lipophilicity has no detrimental effect on antiplasmodial activity (Table 1). The cytotoxicity of the indol-3-one derivatives (CC$_{50}$ 11–164 μM) was relatively low. The hit in this series, compound **7** (IC$_{50}$ = 49 nM; IS = 423.4), carries groups (R^1, R^2) showing that the antiplasmodial activity could be greatly improved by adding an electron-donating group like R^1 and R^2 as substituents. The same substituent effects are observed in the indolone and indolone-*N*-oxide series (Fig. 1, Table 1) giving homologous hits.

3. Conclusion

In conclusion we report the synthesis and the electrochemical behaviour of 2-aryl-3*H*-indol-3-ones, along with the evaluation of their antiplasmodial activity and cytotoxicity. Compound **7** possessed the best activity in this series with an optimum combination of antiplasmodial activity and cytotoxicity (IS = 423). By comparing the results obtained for the two homologous series, deoxygenated (this study) and *N*-oxide (previous results), we observed a parallelism between the effect of substituents, the antiplasmodial activity, the structure of the
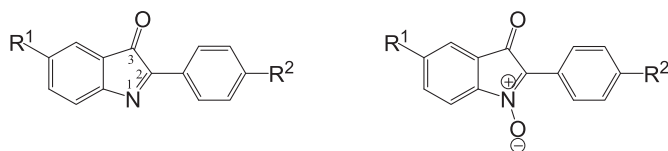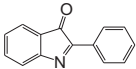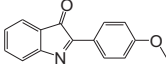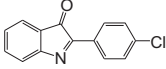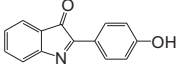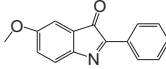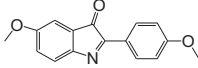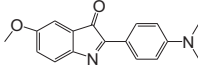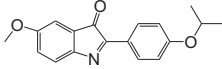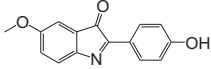
Fig. 1. 2-Aryl-3*H*-indol-3-ones (*left*) and 2-aryl-3*H*-indol-3-one-*N*-oxides (*right*).

Table 1
2-Aryl-3*H*-indol-3-ones: structure, *in vitro* antiplasmodial activity and cytotoxicity.

Compd	Structure	Log P_{calc}[b] (VCCLAB)	IC$_{50}$ (nM) FcB1 strain	CC$_{50}$ (μM)[c] MCF-7	Selectivity index MCF-7/FcB1[d]
1		2.94 (2.06)[a]	1327 ± 24 (889 ± 88)	164 (19.5)	135 (22)
2		2.79 (2.03)	514 ± 287 (195 ± 20)	38 (>39.5)	74 (>202)
3		3.38 (2.68)	192 ± 43 (272 ± 16)	20.3 (17.8)	105 (66)
4		2.83 (1.89)	101 ± 11	130	1289
5		2.80 (2.02)	141 ± 6 (184 ± 53)	21 (13.4)	146 (73)
6		2.64 (2.07)	80 ± 21 (40 ± 39)	30.7 (>35.3)	381.4 (>882)
7		3.01 (2.24)	49 ± 37 (<3)	20.7 (43.9)	423.4 (>14,623)
8		3.51 (2.87)	88 ± 20 (17 ± 2)	11.2 (>32.1)	127 (>1889)
9		2.70 (2.00)	99 ± 36	16	164
Chloroquine		5.28	151 ± 6	19.4	167
Sodium artesunate		2.29	6 ± 3	9.8	1633

[a] Data in parentheses refer to the indolone-*N*-oxide series [4].
[b] Log P_{calc} calculated with VCCLAB (http://www.virtuallaboratory.org/lab/alogps/start.html).
[c] The drug concentration needed to cause a 50% decrease in the cell viability. The IC$_{50}$ SD were always lower than 10% and are not shown for maximum visibility.
[d] Selectivity index was calculated according to the following formula: SI FcB1 = CC$_{50}$ (MCF-7)/IC$_{50}$ (FcB1).

hits, the selectivity index, and the electrochemical behaviour. The deoxygenated series appears slightly less active than the *N*-oxide series; this could originate from the poorer reversibility of the N(1)=C(2) bond at the reduction. Indeed, one of the hypotheses explaining the high antimalarial activity of these compounds may be their ability to be recycled by products of the heme degradation (iron and reactive oxygen species) issuing from the redox metabolism of the parasite in the red blood cell. Further work on this redox recycling and on the antimalarial activity *in vivo* is underway.
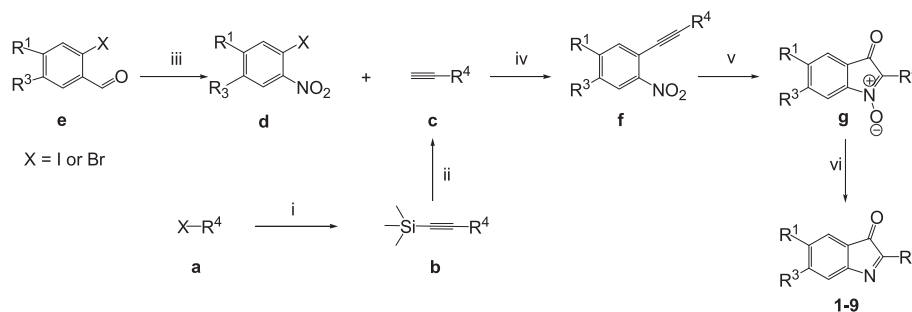
Reagents and conditions: (i) (CH$_3$)$_3$Si-C≡CH, Pd(PPh$_3$)$_2$Cl$_2$, CuI, Et$_3$N, N$_2$, rt; (ii) CH$_3$OH, CH$_2$Cl$_2$, K$_2$CO$_3$; (iii) AcOH, HNO$_3$ fuming; (iv) Pd(PPh$_3$)$_2$Cl$_2$, CuI, NEt$_3$, N$_2$, rt; (v) Pd(CH$_3$CN)$_2$Cl$_2$, CH$_3$CN, N$_2$, reflux 86 °C; and (vi) InCl$_3$, CH$_3$CN, N$_2$, reflux.

Scheme 1. General synthetic route for the indol-3-one derivatives.
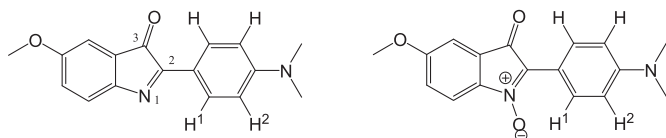
Fig. 2. 2-(4-Dimethylamino-phenyl)-5-methoxy-indol-3-one (7) and 2-(4-dimethylaminophenyl)-5-methoxy-1-oxy-indol-3-one (7′).

4. Experimental

4.1. Chemistry

4.1.1. General

Products **1**, **2**, **3**, **5** and **6** are known and their physical and spectroscopic data were compared with the reported values. Melting points were determined with an Electrothermal 9300 capillary melting point apparatus and are uncorrected. IR spectra were recorded on a Perkin–Elmer PARAGON 1000 FT-IR spectrometer. ^{1}H and ^{13}C NMR spectra were recorded on an AC Bruker spectrometer at 300 MHz (^{1}H) and 75 MHz (^{13}C) using $(CD_3)_2SO$ or $CDCl_3$ as solvents. High resolution mass spectra (HRMS) were recorded on a Bruker Maxis spectrometer (Service Commun Toulouse, France). Silica Gel 60 (Merck 70–230) was used for column chromatography. The progress of the reactions was monitored by thin layer chromatography (TLC) on using Kieselgel 60 F254 (Merck) plates.

4.1.2. General procedure for the deoxygenation of indolone-N-oxides

Anhydrous indium trichloride (0.221 g, 1 mmol) was added to a stirred solution of N-oxide **g** [4] (1 mmol) in acetonitrile (15 mL) and the mixture was refluxed under a nitrogen atmosphere for 3 h. After completion of the reaction (monitored by TLC), the solvent was removed under reduced pressure and the residue was treated with water (50 mL). The resultant mixture was made basic (pH 8) with 25% aqueous ammonia and extracted with dichloromethane, the organic layer dried (Na_2SO_4) and the solvent distilled off to give the crude product, which was purified by column (silica) chromatography (pet. ether/dichloromethane) to afford the corresponding deoxygenated products **1**–**9**.

4.1.2.1. 2-Phenyl-indol-3-one (1) [21].
Red solid, yield: 81%, mp: 99–101 °C. ^{1}H NMR (300 MHz, CDCl$_3$): δ: 7.33–7.36 (m, 1H), 7.48–7.61 (m, 6H), 8.28 (d, J = 8.1 Hz, 2H). IR (KBr, cm^{-1}): 1758, 1720 (C=O), 1534 (C=N), 826, 765. MS-(+)APCI, m/z: 208 [M+H]$^+$.
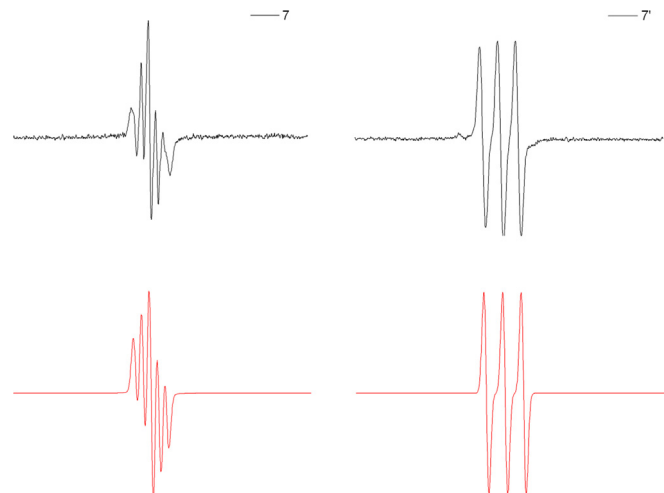

Fig. 4. EPR spectra and the corresponding simulated spectra recorded for compounds **7** and **7′** (2 mmol L^{-1}) during electrolysis at −1 V in ACN containing TBAP (0.1 mol L^{-1}).

HRMS (DCI, CH$_4$) m/z calcd for C$_{14}$H$_{10}$NO [M+H]$^+$ 208.0762. Found 208.0767.

4.1.2.2. 2-(4-Methoxy-phenyl)-indol-3-one (2) [21].
Red solid, yield: 74%, mp: 116–118 °C. ^{1}H NMR (300 MHz, DMSO-d_6): δ: 3.86 (s, 3H, CH$_3$), 7.12 (d, J = 9 Hz, 2H), 7.28–7.33 (m, 1H), 7.43 (d, J = 7.5 Hz, 1H), 7.56–7.65 (m, 2H), 8.28 (d, J = 9 Hz, 2H). IR (KBr, cm^{-1}): 1760, 1722 (C=O), 1536 (C=N), 1258, 1044, 831, 757. MS-(+)APCI, m/z: 238 [M+H]$^+$. HRMS (DCI, CH$_4$) m/z calcd for C$_{15}$H$_{12}$NO$_2$ [M+H]$^+$ 238.0868. Found 238.0859.

4.1.2.3. 2-(4-Chloro-phenyl)-indol-3-one (3) [21].
Red solid, yield: 78%, mp: 124–126 °C. ^{1}H NMR (300 MHz, DMSO-d_6): δ: 7.37–7.66 (m, 6H), 8.28 (d, J = 8.4 Hz, 2H). IR (KBr, cm^{-1}): 1757, 1719 (C=O), 1540 (C=N), 789, 761. MS-(+)APCI, m/z: 242 [M+H]$^+$. HRMS (DCI, CH$_4$) m/z calcd for C$_{14}$H$_9$ClNO [M+H]$^+$ 242.0373. Found 242.0362.

4.1.2.4. 2-(4-Hydroxy-phenyl)-indol-3-one (4).
Brown solid, yield: 65%, mp: 233–235 °C. ^{1}H NMR (300 MHz, DMSO-d_6): δ: 6.93 (d, J = 8.7 Hz, 2H), 7.26–7.31 (m, 1H), 7.39 (d, J = 7.8 Hz, 1H), 7.54–7.64 (m, 2H), 8.20 (d, J = 8.7 Hz, 2H). ^{13}C NMR (75 MHz, DMSO-d_6) δ: 113.1 (×2), 113.2, 121.4, 122.6, 129.0 (×2), 129.3, 130.2, 131.6, 135.2, 147.7, 151.5, 192.6 (C=O). IR (KBr, cm^{-1}): 1757, 1722 (C=O), 1535 (C=N), 830, 758. MS-(+)APCI, m/z: 224 [M+H]$^+$. HRMS (DCI, CH$_4$) m/z calcd for C$_{14}$H$_{10}$NO$_2$ [M+H]$^+$ 224.0712. Found 224.0699.
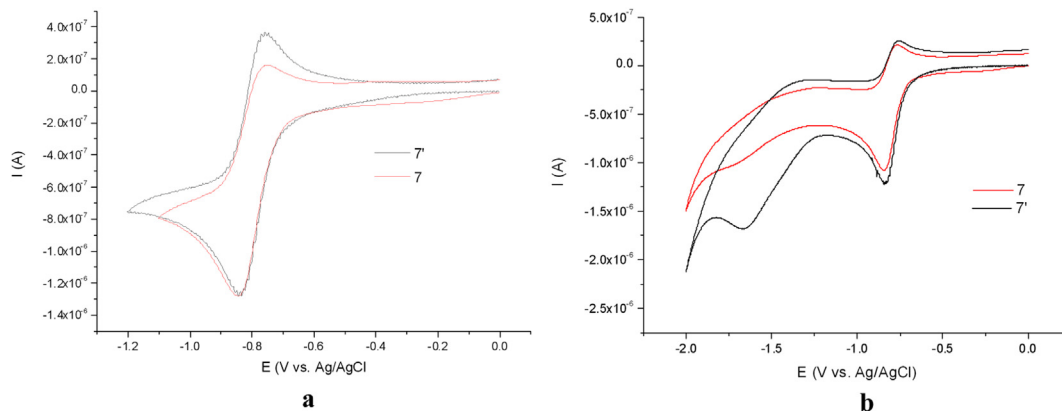
Fig. 3. Cyclic voltammograms in ACN/TBAP 0.1 M of compounds 7 and its oxygenated form 7′, potential scan speed 0.1 V/s.

4.1.2.5. 5-Methoxy-2-phenyl-indol-3-one (5) [22]. Violet solid, yield: 61%, mp: 208–210 °C. ^{1}H NMR (300 MHz, CDCl$_3$): δ: 3.85 (s, 3H, CH$_3$), 6.96–7.00 (m, 1H), 7.11 (d, J = 2.7 Hz, 1H), 7.31 (d, J = 8.1 Hz, 1H), 7.47–7.52 (m, 3H), 8.31 (d, J = 8.1 Hz, 2H). IR (KBr, cm^{-1}): 1762, 1720 (C=O), 1536 (C=N), 768, 690. MS-(+)APCI, m/z: 238 [M+H]$^+$. HRMS (DCI, CH$_4$) m/z calcd for C$_{15}$H$_{12}$NO$_2$ [M+H]$^+$ 238.0868. Found 238.0879.

4.1.2.6. 5-Methoxy-2-(4-methoxy-phenyl)-indol-3-one (6) [22]. Violet solid, yield: 66%, mp: 215–217 °C. ^{1}H NMR (300 MHz, CDCl$_3$): δ: 3.85 (s, 3H, CH$_3$), 3.89 (s, 3H, CH$_3$), 6.96–7.02 (m, 3H), 7.11 (d, J = 3 Hz, 1H), 7.27 (d, J = 9 Hz, 1H), 8.35 (d, J = 9 Hz, 2H). ^{13}C NMR (75 MHz, DMSO-d_6) δ: 55.4, 55.9, 111.2, 114.3 (×2), 120.2, 122.1, 122.9, 124,3, 130.8 (×2), 153.2, 159.4, 159.7, 162.7, 194.4 (C=O). IR (KBr, cm^{-1}): 1759, 1720 (C=O), 1535 (C=N), 831, 756. MS-(+)APCI, m/z: 268 [M+H]$^+$. HRMS (DCI, CH$_4$) m/z calcd for C$_{16}$H$_{14}$NO$_3$ [M+H]$^+$ 268.0974. Found 268.0973.

4.1.2.7. 2-(4-Dimethylamino-phenyl)-5-methoxy-indol-3-one (7). Violet solid, yield: 52%, mp: 189–191 °C. ^{1}H NMR (300 MHz, DMSO-d_6): δ: 3.04 (s, 6H, 2 CH$_3$), 3.80 (s, 3H, CH$_3$), 6.82 (d, J = 9 Hz, 2H), 7.6–7.08 (m, 2H), 7.24 (d, J = 9 Hz, 1H), 8.15 (d, J = 9 Hz, 2H). ^{13}C NMR (75 MHz, DMSO-d_6) δ: 40.1 (2 CH$_3$), 55.4, 11.5 (×2), 116.8, 122.0, 123.3, 125.4, 132.6 (×2), 150.8, 154.3, 159.7, 160.0, 162.6, 193.8 (C=O). IR (KBr, cm^{-1}): 1758, 1725 (C=O), 1538 (C=N), 779, 754, 698. MS-(+)APCI, m/z: 281 [M+H]$^+$. HRMS (DCI, CH$_4$) m/z calcd for C$_{17}$H$_{17}$N$_2$O$_2$ [M+H]$^+$ 281.1290. Found 281.1292.

4.1.2.8. 2-(4-Isopropoxy-phenyl)-5-methoxy-indol-3-one (8). Red solid, yield: 78%, mp: 114–116 °C. ^{1}H NMR (300 MHz, DMSO-d_6): δ: 1.31 (d, J = 6 Hz, 6H, 2 CH$_3$), 3.82 (s, 3H, CH$_3$), 4.74 (m, 1H, CH), 7.05–7.13 (m, 4H), 7.32 (d, J = 8.1 Hz, 1H), 8.19 (d, J = 9 Hz, 2H). ^{13}C NMR (75 MHz, DMSO-d_6) δ: 22.3 (2 CH$_3$), 55.3, 69.1, 111.0, 114.8 (×2), 119.8, 121.6, 122.9, 124.3, 130.8 (×2), 154.4, 160.5, 160.7, 162.8, 193.7 (C=O). IR (KBr, cm^{-1}): 1756, 1722 (C=O), 1538 (C=N), 836, 762. MS-(+)APCI, m/z: 296 [M+H]$^+$. HRMS (DCI, CH$_4$) m/z calcd for C$_{18}$H$_{18}$NO$_3$ [M+H]$^+$ 296.1287. Found 296.1289.

4.1.2.9. 2-(4-Hydroxy-phenyl)-5-methoxy-indol-3-one (9). Violet solid, yield: 55%, mp: >300 °C. ^{1}H NMR (300 MHz, DMSO-d_6): δ: 3.82 (s, 3H, CH$_3$), 6.91 (d, J = 9 Hz, 2H), 7.12–7.13 (m, 2H), 7.31 (d, J = 8.1 Hz, 1H), 8.14 (d, J = 9 Hz, 2H). ^{13}C NMR (75 MHz, DMSO-d_6) δ: 55.4, 110.9, 114.7 (×2), 120.1, 121.9, 122.7, 124.4, 131.1 (×2), 153.3, 159.5, 160.0, 162.5. 194.3 (C=O). IR (KBr, cm^{-1}): 1762, 1721 (C=O), 1546 (C=N), 782, 761. MS-(+)APCI, m/z: 254 [M+H]$^+$. HRMS (DCI, CH$_4$) m/z calcd for C$_{15}$H$_{12}$NO$_3$ [M+H]$^+$ 254.0817. Found 254.0825.

4.2. Electrochemistry

Experiments were carried out at 25 °C in acetonitrile containing tetrabutyl ammonium perchlorate, TBAP 0.1 mol L^{-1}, using an Autolab (Methrom) and a conventional cell with three electrodes: reference electrode: a double junction electrode with the AgCl/Ag couple in KCl 3 M; counter electrode: a platinum electrode sheet (5 × 5 mm); working electrode: a platinum disk (0.5 mm diameter) for cyclic voltammetry and a rotating disk electrode (EDI, Tacussel) for stationary conditions. All solutions were deoxygenated (argon bubbling, 15 min) and a blanket of the inert gas was maintained during the experiment. Voltamperograms were recorded for a compound concentration around 10^{-3} mol L^{-1} (ferrocene or indolone) and a potential scan rate ranging from 0.02 V/s up to 100 V/s depending on experiments.

4.3. EPR spectroelectrochemical analysis

The EPR spectrometer was coupled to a Voltalab 80 PGZ 402 (Radiometer). A flat quartz cell adapted to electrochemical measurements (Bruker, Wissembourg, France) was used for analysis. The electrochemical reduction was performed using a three-electrode set-up: the working and counter-electrode were platinum and the reference electrode was a silver wire. The applied potential was chosen to be on the diffusion plateau of the first reduction wave obtained under stationary conditions: Eapplied = E$_{1/2}$ − 0.2 V. The electrolysis potential was applied to the solution containing the test compound in acetonitrile/TPAB and the EPR spectra were immediately recorded as a function of time. EPR spectra were obtained at X-band at room temperature on a Bruker EMX-8/2.7 (9.86 GHz) equipped with a high-sensitivity cavity (4119/HS 0205) and a gaussmeter (Bruker). WINEPR and SIMFONIA software (Bruker) were used for processing the EPR data and computer simulations spectra. Typical scanning parameters were: scan rate, 1.2 G/s; scan number, 1; modulation amplitude, 1 G; modulation frequency, 100 kHz; microwave power, 20 mW; sweep width, 100 G; sweep time, 83.88 s; time constant, 40.96 ms; centre field, 3480 G; receiver gain, 1×10^5.

4.4. Biology

4.4.1. In vitro antiplasmodial activity

The FcB1 strain of *P. falciparum* (chloroquine-resistant strain) was maintained in RPMI 1640 medium (BioWhittaker, Cambrex, Belgium) containing L-glutamine (BioWhittaker), 25 mM HEPES (BioWhittaker), and 10% human serum (EFS, Toulouse, France) as previously described [23]. Parasitized RBCs were maintained in 25 cm^2 culture flasks (TPP, Switzerland) in a controlled atmosphere (5% CO$_2$, 100% relative humidity) and synchronized by a combination of magnetic enrichment followed by D-sorbitol lysis [24,25]. Chloroquine was dissolved in culture medium and sodium artesunate in ethanol (stock solutions: 10 mg/mL). The stock solutions of the tested drugs were prepared by mixing 1 mg of drug in 1 mL DMSO and adding it to a solution of 1 mg BSA in 1 mL of RPMI medium, giving a stock solution at 0.5 mg/mL. For the drug assays, serial drug dilutions were made in *P. falciparum* culture media and added to 96-well (TPP) culture plates. For the evaluation of *Plasmodium* growth inhibition, the culture was plated in 96-well plates as described elsewhere [4]. [^{3}H]-Hypoxanthine (Perkin−Elmer) was added 24 h after the beginning of incubation. At the end of the incubation (48 h), the microtiter plates were frozen and thawed, and each well was harvested onto glass-fibre filter paper. The [^{3}H]-hypoxanthine incorporation was determined with a β-counter (1450-Microbeta Trilux, Wallac-PerkinElmer). Growth inhibition percentages were plotted as a semilogarithmic function of drug concentration. The IC$_{50}$ values were determined by linear regression analysis on the linear segments of the curves. In each assay, drugs were tested in triplicate and assays were repeated three times. Controls were carried out to assess the background (negative control) and parasite growth (positive control).

4.4.2. In vitro cytotoxicity assay

Cytotoxicity was determined on human breast cancer cells (MCF7). The cells were cultured in the same conditions as those used for *P. falciparum*, except that 10% human serum was replaced by 10% foetal calf serum (Cambrex). After trypsinization, cells were distributed in 96-well plates at 2×10^4 cells/well in 100 μL of culture medium. After an overnight incubation 100 μL culture medium containing the tested compounds at various concentrations (the final concentrations in the wells were 1, 10, and 100 μg mL^{-1}) was added. Cell growth inhibition was estimated by a colorimetric assay

based on XTT reduction after a 48 h contact between drugs and cells [26]. Experiments were performed twice in triplicate.

Appendix A. Supplementary data

Supplementary data related to this article can be found at http://dx.doi.org/10.1016/j.ejmech.2014.03.059.

References

[1] WHO: World Malaria Report, 2012. http://www.who.int/malaria/publications/world_malaria_report_2012/report/en/.
[2] W.A. Guiguemde, A.A. Shelat, J.F. Garcia-Bustos, T.T. Diagana, F.J. Gamo, R.K. Guy, Global phenotypic screening for antimalarials, Chemistry & Biology 19 (2012) 116–129.
[3] F.J. Gamo, L.M. Sanz, J. Vidal, C. de Cozar, E. Alvarez, J.L. Lavandera, D.E. Vanderwall, D.V.S. Green, V. Kumar, S. Hasan, J.R. Brown, C.E. Peishoff, L.R. Cardon, J.F. Garcia-Bustos, Thousands of chemical starting points for antimalarial lead identification, Nature 465 (2010) 305–310.
[4] F. Nepveu, S. Kim, J. Boyer, O. Chatriant, H. Ibrahim, K. Reybier, M.C. Monje, S. Chevalley, P. Perio, B.H. Lajoie, J. Bouajila, E. Deharo, M. Sauvain, R. Tahar, L. Basco, A. Pantaleo, F. Turrini, P. Arese, A. Valentin, E. Thompson, L. Vivas, S. Petit, J.P. Nallet, Synthesis and antiplasmodial activity of new indolone-N-oxide derivatives, Journal of Medicinal Chemistry 53 (2010) 699–714.
[5] N. Ibrahim, H. Ibrahim, S. Kim, J.P. Nallet, F. Nepveu, Interactions between antimalarial indolone-N-oxide derivatives and human serum albumin, Biomacromolecules 11 (2010) 3341–3351.
[6] N. Ibrahim, H. Ibrahim, J. Dormoi, S. Briolant, B. Pradines, A. Moreno, D. Mazier, P. Legrand, F. Nepveu, Albumin-bound nanoparticles of practically water-insoluble antimalarial lead greatly enhance its efficacy, International Journal Pharmaceutics 64 (2014) 214–224.
[7] K. Reybier, H.Y. Nguyen Thi, H. Ibrahim, P. Perio, A. Montrose, P.L. Fabre, F. Nepveu, Electrochemical behavior of indolone-N-oxides: relationship to structure and antiplasmodial activity, Bioelectrochemistry 88 (2012) 57–64.
[8] H.Y. Nguyen Thi, H. Ibrahim, K. Reybier, P. Perio, F. Souard, E. Najahi, P.L. Fabre, F. Nepveu, Pro-oxidant properties of indolone-N-oxides in relation to their antimalarial properties, Journal of Inorganic Biochemistry 126 (2013) 7–16.
[9] H. Ibrahim, A. Pantaleo, F. Turrini, P. Arese, J.P. Nallet, F. Nepveu, Pharmacological properties of indolone-N-oxides controlled by a bioreductive transformation in red blood cells, Medicinal Chemistry Communications 2 (2011) 860–869.
[10] A. Pantaleo, E. Ferru, R. Vono, G. Girbaldi, O. Lobina, F. Nepveu, H. Ibrahim, J.P. Nallet, F. Carta, F. Mannu, P. Pippia, E. Campanella, P.S. Low, F. Turrini, New antimalarial indolone-N-oxides, generating radical species, destabilize the host cell membrane at early stages of Plasmodium falciparum growth: role of band 3 tyrosine phosphorylation, Free Radical Biology and Medicine 52 (2012) 527–536.
[11] D. Belorgey, D.A. Lanfranchi, E. Davioud-Charvet, 1,4-Naphthoquinones and other NADPH-dependent glutathione reductase-catalyzed redox cyclers as antimalarial agents, Current Pharmaceutical Design 19 (2013) 2512–2528.
[12] F. Nepveu, F. Turrini, Targeting the redox metabolism of P. falciparum, Future Medicinal Chemistry 16 (2013) 1993–2006.
[13] C.V. Ramana, P. Patel, K. Vanka, B. Miao, A. Degterev, A combined experimental and density functional theory study on the Pd-mediated cycloisomerization of o-alkynylnitrobenzenes – synthesis of isatogens and their evaluation as modulators of ROS-mediated cell death, European Journal of Organic Chemistry (2010) 5955–5966.
[14] H. Ibrahim, A. Furiga, E. Najahi, C.P. Hénocq, J.P. Nallet, C. Roques, A. Aubouy, M. Sauvain, P. Constant, M. Daffe, F. Nepveu, Antibacterial, antifungal and antileishmanial activities of indolone-N-oxide derivatives, Journal of Antibiotics 60 (2012) 1–6.
[15] M. Ilias, D.C. Barman, D. Prajapati, J.S. Sandhu, An indium mediated efficient chemoselective deoxygenation of N-oxides and nitrones, Tetrahedron Letters 43 (2002) 1877–1879.
[16] E. Najahi, A. Valentin, N. Téné, M. Treilhou, F. Nepveu, Synthesis and biological evaluation of new bis-indolone-N-oxides, Bioorganic Chemistry 48 (2013) 18–21.
[17] D.W. Price, S.M. Dirk, F. Maya, J.M. Tour, Improved and new syntheses of potential molecular electronics devices, Tetrahedron 59 (2003) 2497–2518.
[18] E.C. Keske, O.V. Zenkina, R. Wang, C.M. Crudden, Synthesis and structure of silver and rhodium 1,2,3-triazol-5-ylidene mesoionic carbene complexes, Organometallics 31 (2012) 456–461.
[19] M. Joshi, M. Patel, R. Tiwari, A.K. Verma, Base-mediated selective synthesis of diversely substituted N-heterocyclic enamines and enaminones by the hydroamination of alkynes, Journal of Organic Chemistry 77 (2012) 5633–5645.
[20] ALOGPS 21. http://www.virtuallaboratory.org/lab/alogps/ (accessed 10–11.07.09.).
[21] L. Ke-Qing, Synthesis of 2-aryl-3H-indol-3-ones via trapping reaction in singlet oxygenation of 2-arylindoles, Chinese Journal of Chemistry 14 (1996) 259–264.
[22] J. Schmitt, C. Perrin, M. Langlois, M. Suquet, I. Indoles, Preparation of substituted 2-aryl-3H-indol-3-ones, Bulletin de la Societe Chimque de France 4 (1969) 1227–1234.
[23] N. Cachet, F. Hoakwie, S. Bertani, G. Bourdy, E. Deharo, D. Stien, E. Houel, H. Gornitzka, J. Fillaux, S. Chevalley, A. Valentin, V. Jullian, Antimalarial activity of simalikalactone E, a new quassinoid from Quassia amara L. (Simaroubaceae), Antimicrobial Agents and Chemotherapy 53 (2009) 4393–4398.
[24] C. Ribaut, A. Berry, S. Chevalley, K. Reybier, I. Morlais, D. Parzy, F. Nepveu, F.F. Benoit-Vical, A. Valentin, Concentration and purification by magnetic separation of the erythrocytic stages of all human Plasmodium species, Malaria Journal 7 (2008) 45.
[25] C. Lambros, J.P. Vanderberg, Synchronization of Plasmodium falciparum erythrocytic stages in culture, Journal of Parasitology 65 (1979) 418–420.
[26] B. Portet, N. Fabre, V. Roumy, H. Gornitzka, G. Bourdy, S. Chevalley, M. Sauvain, A. Valentin, C. Moulis, Activity-guided isolation of antiplasmodial dihydrochalcones and flavanones from Piper hostmannianum var. berbicense, Phytochemistry 68 (2007) 1312–1320.